Modelling of Seismic and Resistivity Responses during the Injection of CO2 in Sandstone Reservoir

Muhamad Nizarul Idhafi Bin Omar [1], Luluan Almanna Lubis [1], Muhammad Nur Arif Zanuri[1], Deva P. Ghosh[1], Sonny Irawan[2], Shiferaw Regassa Jufar[2]
Geoscience Department, Universiti Teknologi PETRONAS, 31750 Tronoh, Perak, Malaysia.
E-mail: nizarulidhafi@gmail.com

Abstract: Enhanced oil recovery plays vital role in production phase in a producing oil field. Initially, in many cases hydrocarbon will naturally flow to the well as respect to the reservoir pressure. But over time, hydrocarbon flow to the well will decrease as the pressure decrease and require recovery method so called enhanced oil recovery (EOR) to recover the hydrocarbon flow. Generally, EOR works by injecting substances, such as carbon dioxide (CO2) to form a pressure difference to establish a constant productive flow of hydrocarbon to production well. Monitoring CO2 performance is crucial in ensuring the right trajectory and pressure differences are established to make sure the technique works in recovering hydrocarbon flow. In this paper, we work on computer simulation method in monitoring CO2 performance by seismic and resistivity model, enabling geoscientists and reservoir engineers to monitor production behaviour as respect to CO2 injection.

1. Introduction

Greenhouse gases has become an attention as the main cause of global warming. Due to global warming, reduction technologies for CO2, the most abundant greenhouse gas, become an urgent business. Kyoto Protocol (1997) defined an implementation goal that most of the world's countries could reduce CO2 emission by 5.2% of the 1990 totals. Prior to this, underground storage of carbon dioxide was introduced to reduce the effect of greenhouse gases to help in slowing down global warming [1].

The abundant of greenhouse gases often linked with fossil energy sources exploration, production and usage [2]. The carbon capture and storage (CCS) project, targeting on reducing CO2 in the atmosphere works by storing captured CO2 into geologic structure, such as large sedimentary basins in Illinois, Michigan and Western Canadian sedimentary basin [3]. In oil and gas exploration, the CO2 instead of being stored in large basins, also been widely used in enhanced oil recovery (EOR) to retrieve the recovered oil by performing a pressure difference to enable hydrocarbon migration to producing wells.

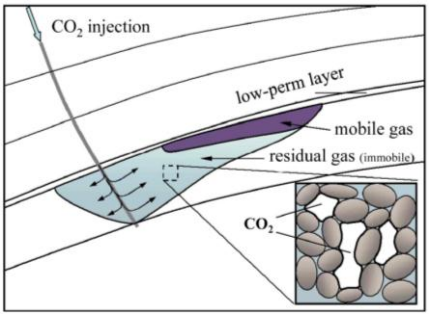

Figure 1.1: CO2 stored in saline aquifer for CCS project [4]

[1] Geosciences Department, Universiti Teknologi PETRONAS, Malaysia, Bandar Seri Iskandar, 32610, Tronoh, Perak Darul Ridzuan, Malaysia
[2] Petroleum Engineering Department, Universiti Teknologi PETRONAS, Malaysia, Bandar Seri Iskandar, 32610, Tronoh, Perak Darul Ridzuan, Malaysia

The method, by using CO2 in many cases is the most cost effective method to extract the final amounts of recoverable oil from depleted field [5] which share the same technology as carbon capture and storage (CCS) in term of development and monitoring [3]. Despite being conceptually the same, when implemented in EOR, the seismic and resistivity respond of the CO2 will not be the same as in CCS, where the CO2 now will be in contact with hydrocarbon to lead the recovery effort.

1.1 Enhanced Oil Recovery (EOR)

For over 40 years, injecting CO2 to tertiary reservoirs has been widely accepted as an effective method in enhanced oil recovery (EOR) [6]. Since October 1996, Statoil and its Sleipner partners working on Utsira Sand, offshore Norway have injected CO2 about 200 meter below reservoir top [1]. In Gullfaks Field in the North Sea, by injecting CO2 instead of water for EOR, significant amount of extra oil can be retrieved [7]. By using CO2 as an alternative for EOR, the majority of previous and current CO2 EOR projects has high economic return in high gas utilization efficiencies (167-227 cm^2 CO2/STB oil) [6].

In environmental perspective, the potential of CO2 storage combining with EOR is high, up to 60% of injected CO2 can be retained in the reservoir at the CO2 breakthrough if reinjection is not considered [6] . The criteria for suitable reservoir selection for CO2 EOR has been developed in [6].

Table 1.1: Optimum reservoir parameters and weighting factors for ranking oil reservoirs suitable for CO2 EOR [6].

Reservoir parameters	Optimum values	Parametric weight
API Gravity (°API)	37	0.24
Remaining oil saturation	60%	0.20
Pressure over MMP (MPa)	1.4	0.19
Temperature (°C)	71	0.14
Net oil thickness (m)	15	0.11
Permeability (mD)	300	0.07
Reservoir dip	20	0.03
Porosity	20%	0.02

1.2 Resistivity responds of CO2 injected sandstone

Electrical log has been widely used to provide quantitative correlation in exploitation of oil and gas reservoirs to provide an indication on the reservoir content [8]. Direct measurement of geophysical data during CO2 injection are not applicable due to technical and cost issues [9]. Therefore, indirect measurement consist of time lapse survey, resistivity as well as gravity were applied later on. The resistivity value is based on Archie's Law [8] generally will increase as CO2 concentration increase. This is due to resistance built up when more CO2 is added causing harder for the current to flow through the reservoir. The increment trend can be seen following the experiment in [10] [11] [12].

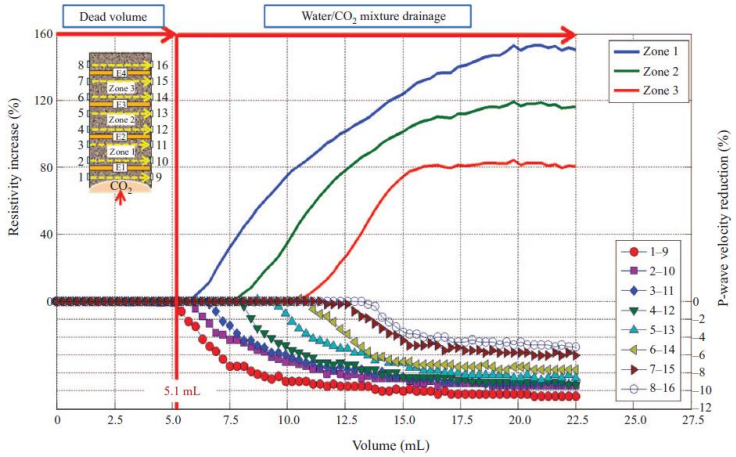

Figure 1.2: Changes in resistivity and P-wave velocities for three zones after CO2 injection. Note the increasing trend of resistivity as CO2 volume increase [10].

1.3 Seismic monitoring on CO2 injection in EOR

4D seismic exploration or time lapse reservoir monitoring (eg: Figure 1.3) has advanced rapidly over the past 10 years to monitor the progress of the injected fluid fronts (eg: water, gas, CO2, etc.) that can save hundreds of millions of dollars in optimizing injection programs [13]. A pilot project in Nagaoka was conducted and revealed after the injection of CO2, the maximum velocity experience 3.0% reduction after injecting 3200 t of CO2 and 3.5 % after injecting 6200 t of CO2 [14]. Notice that the increment of volume of CO2 injected were increased about two times, but the velocity reduction do not increase significantly.

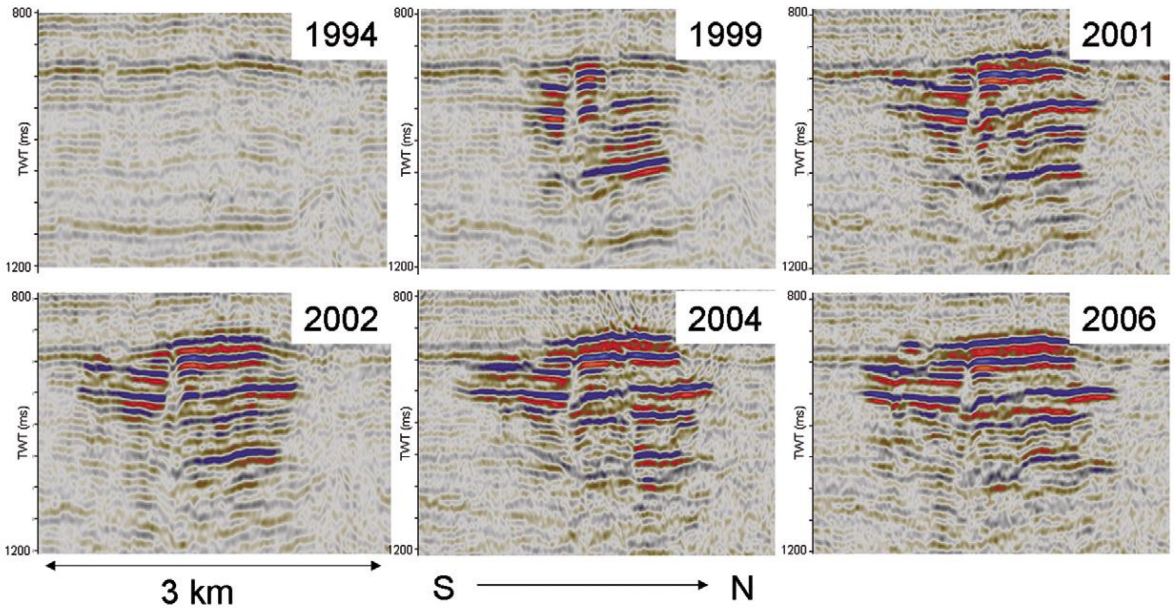

Figure 1.3: The development of CO2 plume over time, studied using time lapse seismic survey [1]

1.4 Elastic Bound

To have a more rational velocity-porosity relations, the gap between well logs and cores with geologic model, rock physics diagnostic analysis is used [15]. Expressed based on Hooke's Law [16], the elastic behavior of rock and the pore fluid become the fundamental of rock physics. Gassmann's fluid substitution theorem widely used to relates rock with fluid under three major assumptions: the rock is homogeneous and isotropic, the pore space is completely connected and the fluids are movable [17].

While many models proposed include complicated inputs, Gassmann relations reflect the changes in P and S wave velocity as accordance to saturation changes with simpler inputs. Density and P wave velocity logs are initial inputs and the imported parameter during substitution are matrix bulk modulus (Kmatrix), frame or dry rock bulk modulus (Krock), porosity (ø) and rock shear modulus (G) [18].

$$\frac{K_{\text{sat}}^{(2)}}{K_{\text{mineral}}-K_{\text{sat}}^{(2)}}-\frac{K_{\text{fluid}}^{(2)}}{\phi(K_{\text{mineral}}-K_{\text{fluid}}^{(2)})}=\frac{K_{\text{sat}}^{(1)}}{K_{\text{mineral}}-K_{\text{sat}}^{(1)}}-\frac{K_{\text{fluid}}^{(1)}}{\phi(K_{\text{mineral}}-K_{\text{fluid}}^{(1)})}$$

Fluid substitution formula by Gassmann [17] (1.1).

Since the shear modulus is insensitive to fluid changes, it will remain constant during the substitution [18].

Table 1.2: Elastic and electromagnetic properties of some elements [19].

Medium	K (GPa)	μ (GPa)	ρ (g/cm^3)	R (μm)	η (Pa s)	σ (S/m)
Clay	25	20	2.65	1	–	0.2
Sand grains	39	40	2.65	50	–	0.01
Brine	2.25	0	1.03	–	0.0012	12
CO_2	0.025	0	0.5	–	0.00002	0

$\phi = 25\%$, $r_1 = 10$ cm.

In order to substitute fluids it is necessary to establish their properties. In this case, the two fluids in discussion are water (or brine) and CO2. Density and bulk modulus values (eg: Table 1.2) could be obtained from laboratory measurements but in most of the cases some empirical relations are used such as the equations of Batzle and Wang [20]. These yield the density and bulk modulus knowing temperature, pressure, gravity of the fluid (°API in oil) and concentration (ppm in brine). With these input values, a good approximation of fluid properties can be made at certain conditions. Some researchers caution that using the Batzle and Wang [20] equations as well Gassmann relations (1.1) [17] which were developed for a gas-oil-water scenario, might not represent the reality of a CO2 fluid substitution.

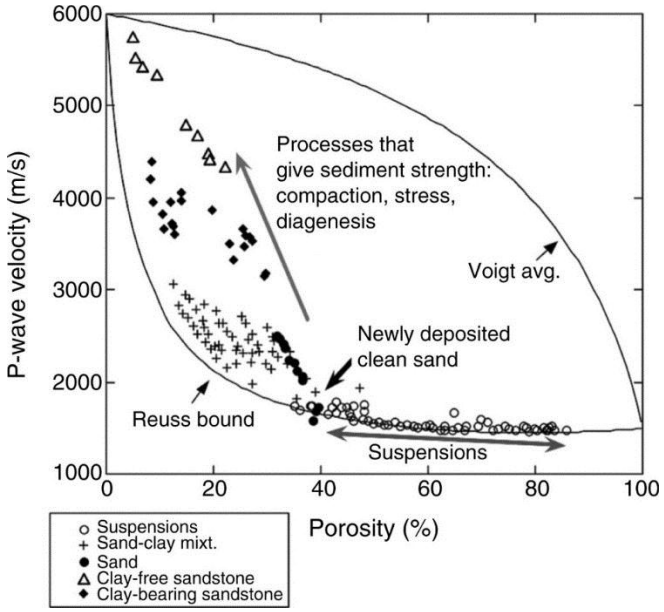

Figure 1.4: Voigt-Reuss upper and lower bound [21]

Fluid bulk modulus and fluid density will manifest the fluid substitution changes and therefore, they will affect the model and define the variations in parameters for seismic modelling. To establish matrix characteristics, one that needs to determine the matrix bulk modulus (Kbulk). These values are tabulated for main mineral components such as quartz and calcite among others. Most of the time, the matrix is composed of different kinds of minerals, and in case that fractional content information is available, the bulk modulus can be calculated using Voigt-Reuss-Hill (VRH) equation [22]. It is possible to obtain the bulk modulus (Kvrh) using Voigt and Reuss bulk modulus respectively (Kvoigt and Kreuss) [18]:

$$K_{bulk} = \frac{1}{2}(K_{voigt} + K_{reuss}) \quad (1.2)$$

$$K_{reuss} = \left[\frac{F_1}{K_1} + \frac{F_2}{K_2}\right]^{-1} \quad (1.3)$$

$$K_{voigt} = [F_1 K_1 + F_2 K_2] \quad (1.4)$$

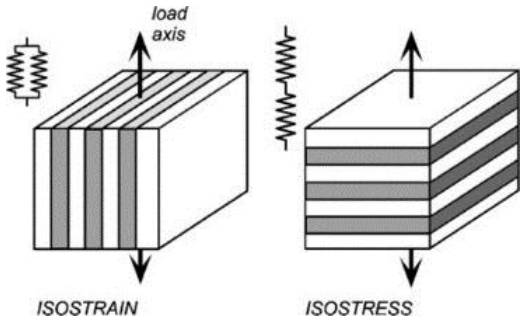

Figure 1.5: Voigt (isostrain) and Reuss (isostress) illustration [22].

2. Methodology

2.1 Homogeneous Core Simulation

To study the P-wave velocity, amplitude and resistivity variation when CO2 is injected to sandstone sample, we use computer simulation based on cylindrical sample of Berea sandstone (50 mm in diameter and 100 mm in length, 19% porosity) [10] as a reference value.

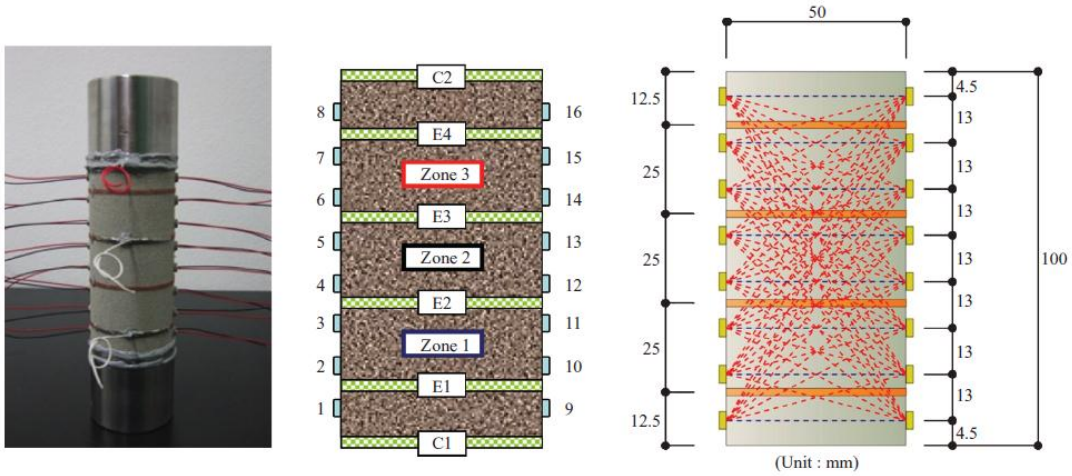

Figure 2.1: Configuration of piezoelectric transducers and electrodes with Berea sandstone sample for seismic velocity and resistivity measurements, respectively. The figure indicates the zone utilized for resistivity measurements as well as a diagram of ray paths for P-wave velocity measurements and P-wave velocity tomography [10].

Two flat current electrodes, 50mm diameter, were attached at the top and the bottom of the sample, and four ring-shaped potential electrodes of 2.5mm width were attached to the sample's surface at a spacing of 25 mm and made as an array. These electrodes are made of copper mesh coated with silver, which to avoid corrosion due to contact with acid.

For seismic value monitoring, our equipment setting were different from [10]. We use a coupled transducer which will be source and receiver on both end of the sample. To have a more realistic data value with reservoir condition, the experimental setup is made as in [10]. Note that the Berea sandstone will be in water saturated and later in oil saturated condition. The measured value (for water-CO2 fluid substitution) will be cross checked with values from Vera [23].

CO2 injection is monitored in time and saturation, and the resultant changes in resistivity and P-wave and S-wave values will be recorded. At the end of the experiments, we wish to obtain updated experimental result as in [10] by computer simulation for homogeneous media.

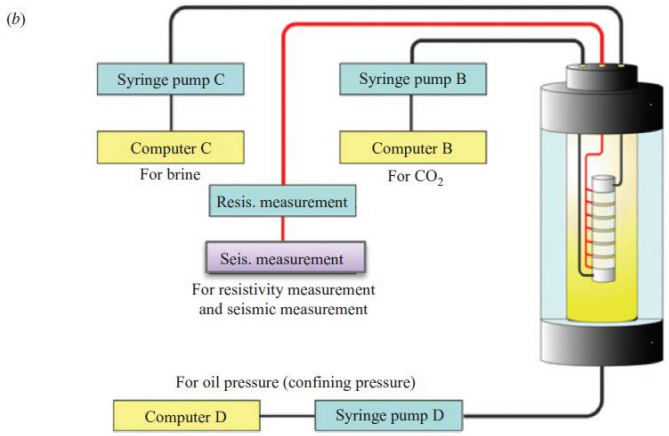

Figure 2.2: Configuration of experimental setup (a) and measurement setup (b) [10]

For the computer simulation, we developed a Python language programmed using hybrid Python version IDE, named Anaconda, first for homogeneous media. The purpose of the simulation is to generate expected result, with total control on the rock properties parameter, to enable us to measure variable range of rock properties rather than to rely on a single core sample.

The following setup is for 4 layers modelling:

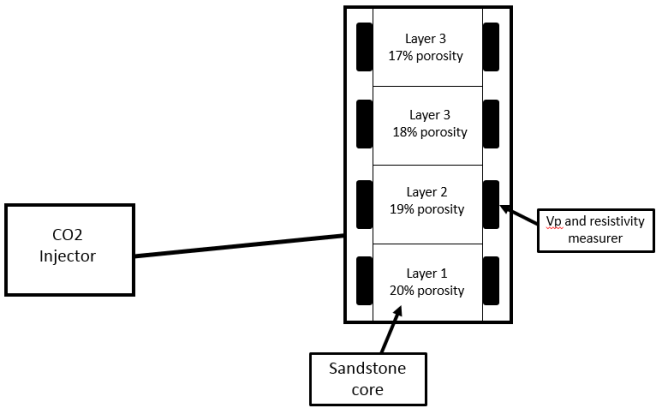

For the purpose of our experiment, based on [10] we developed a core model with parameters as follows:

Table 2.1: Core model parameters

Parameters	Sandstone	Brine	Gas
Bulk Modulus (GPA)	39	3.0	0.038
Shear Modulus (GPA)	44	-	-
Density (g/cc)	2.65	1.039	0.15
Resistivity (ohm.m)	15	1.0	30
Cementation Factor (m)	1.59	-	-
Biot Coefficient	2.0	-	-

The volume of 100% CO2 saturation in the core was set to be 20 mL for each layer, with rate of injection of 0.005 mL/min. The first layer to second layer is 50 min after. The numerical methods to calculate the velocity and resistivity of the simulation are as follows:

Vp calculation:

1. Calculation of matrix modulus by Krief et al. method.
2. Calculation of dry and brine saturated formations by Biot-Gassmann formula.
3. Mix the gas and brine fluids modulus based on their saturation by using Wood's formula to get effective fluid modulus.
4. Repeat Biot-Gassmann and use effective fluids calculated.

Resistivity calculation

1. By matrix modulus, gain porosity extrapolation from brine velocity by Gassmann formula for each brine saturation percentage.
2. Calculate brine saturated resistivity from CRIM formula.
3. By brine modulus, repeat porosity extrapolation from mix fluids (brine-gas) velocity by Gassmann formula.
4. Using brine saturated resistivity, repeat CRIM formula to calculate mix fluids saturated resistivity.

3. Result and Discussion

3.1 Core simulation results

We acquire the simulation result using Anaconda programming IDE, based on Python 2.7 architecture. The results of the heterogeneous core sampling and comparison with our simulation (homogeneous media) are as follows.

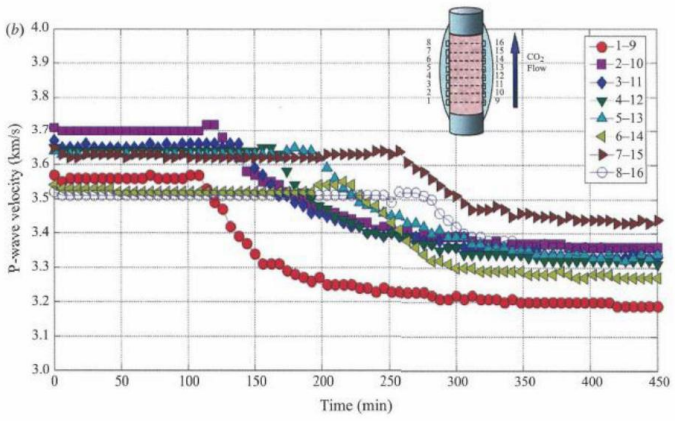

Figure 3.1: Time variation of velocity by injection of supercritical CO2 into water saturated Berea Sandstone in heterogeneous media [10]

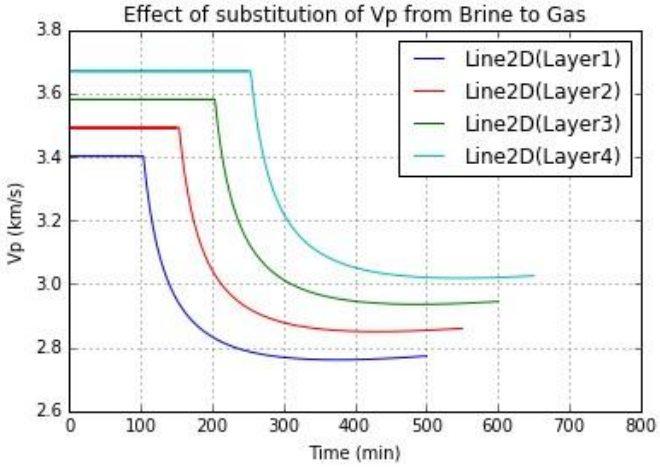

Figure 3.2: The effect of substitution of Vp from brine to CO2 gas in homogeneous media simulation.

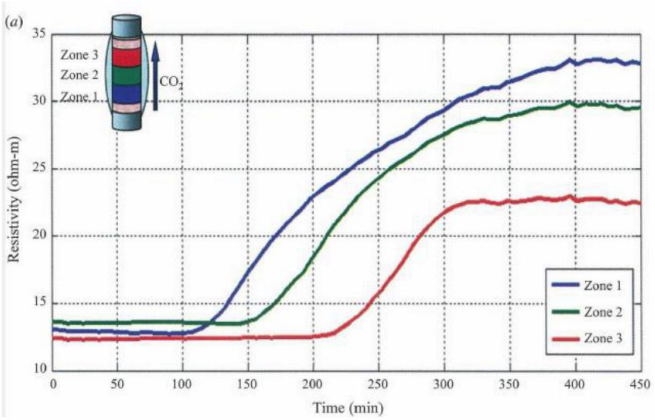

Figure 3.3: Time variation of resistivity by injections of supercritical CO2 into water saturated Berea sandstone in heterogeneous media [10]

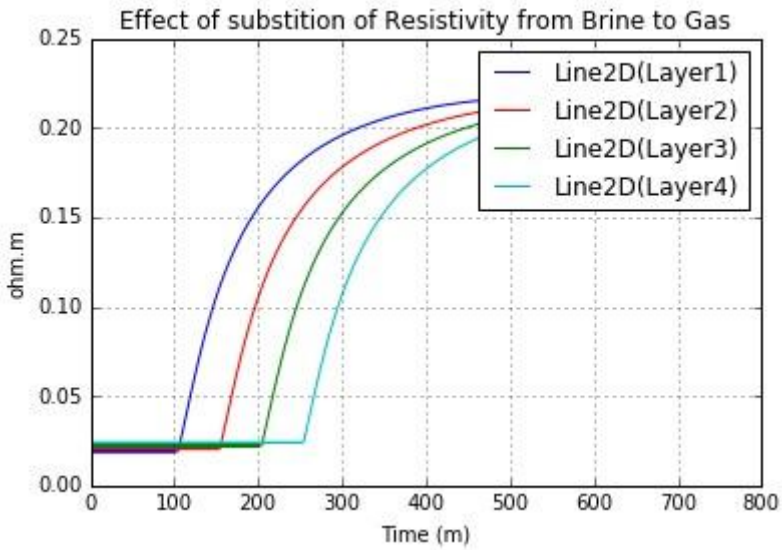

Figure 3.4: Effect of substitution of resistivity from brine to gas in homogeneous media simulation.

Our simulation shows the same trend with established work by [10] although our simulation work is applied on homogeneous media while Kim et al. [10] work is applied on core sample which has heterogeneity included. Therefore, we can conclude that our simulation method can be used in further work to monitor CO2 injection in sandstone using seismic and resistivity method. By having a computer simulation method, we can have a wide range of prediction on the CO2 effect on seismic as well as resistivity value. Rather than to rely on core sampling in laboratory, we can now predict the expected value of seismic and resistivity in a controlled environment with a low cost, fast and robust method.

4. Conclusions

Despite seismic data quality improvements and excellent well control, to achieve correct interpretation, rock physics is required to quantify the connection between geology and seismic data [15]. It is noted from [10] that the seismic sensitivity in detecting CO2 will be not significant after it reach 20% saturation, therefore resistivity value which remain in steady trend of increment will be an alternative once more CO2 volume is added to the reservoir. We have demonstrated that our simulation which is first done for homogeneous media will be a great tool in expecting the outcome in monitoring CO2 EOR using seismic and resistivity. However, we need to extend the research towards heterogeneous media simulation as the real geology often seen as heterogeneous.

References

1. Arts, R., et al., *Ten years' experience of monitoring CO2 injection in the Utsira Sand at Sleipner, offshore Norway.* First break, 2008. **26**(1).
2. Arts, R. and V. Vandeweijer, *The challenges of monitoring CO 2 storage.* The Leading Edge, 2011. **30**(9): p. 1026-1033.
3. Couëslan, M., et al., *Monitoring CO2 injection for carbon capture and storage using time-lapse 3D VSPs.* The Leading Edge, 2013. **32**(10): p. 1268-1276.
4. Juanes, R., et al., *Impact of relative permeability hysteresis on geological CO2 storage.* Water Resources Research, 2006. **42**(12).
5. Chapel, D.G., C.L. Mariz, and J. Ernest. *Recovery of CO2 from flue gases: commercial trends*. in *Canadian Society of Chemical Engineers Annual Meeting*. 1999.
6. Gozalpour, F., S. Ren, and B. Tohidi, *CO2 EOR and storage in oil reservoir.* Oil & gas science and technology, 2005. **60**(3): p. 537-546.
7. Berger, B., O. Kaarstad, and H.A. Haugen. *Creating a large-scale CO2 infrastructure for enhanced oil recovery*. in *Proceedings of the 7th International Conference on Greenhouse Gas Control Technologies, Vancouver, Canada. http://uregina. ca/ghgt7/PDF/papers/nonpeer/108. pdf*. 2004.
8. Archie, G.E., *The electrical resistivity log as an aid in determining some reservoir characteristics.* Transactions of the AIME, 1942. **146**(01): p. 54-62.
9. Park, J., et al. *Feasibility Study on Seismic and CSEM Monitoring of CO2 Injection Based on Laboratory Acoustic and Resistivity Measurement*. in *The Third Sustainable Earth Sciences Conference & Exhibition*. 2015.
10. Kim, J., T. Matsuoka, and Z. Xue, *Monitoring and detecting CO2 injected into water-saturated sandstone with joint seismic and resistivity measurements.* Exploration Geophysics, 2011. **42**(1): p. 58-68.
11. Frohlich, R.K. and C.D. Parke, *The electrical resistivity of the vadose zone—field survey.* Groundwater, 1989. **27**(4): p. 524-530.
12. JafarGandomi, A. and A. Curtis, *Detectability of petrophysical properties of subsurface CO 2-saturated aquifer reservoirs using surface geophysical methods.* The Leading Edge, 2011. **30**(10): p. 1112-1121.
13. Lumley, D.E., *Time-lapse seismic reservoir monitoring.* Geophysics, 2001. **66**(1): p. 50-53.

14. Saito, H., et al., *Time-lapse crosswell seismic tomography for monitoring injected CO2 in an onshore aquifer, Nagaoka, Japan.* Exploration Geophysics, 2006. **37**(1): p. 30-36.
15. Avseth, P., T. Mukerji, and G. Mavko, *Quantitative seismic interpretation: Applying rock physics tools to reduce interpretation risk*. 2005: Cambridge university press.
16. Sokolnikoff, I.S. and R.D. Specht, *Mathematical theory of elasticity*. Vol. 83. 1956: McGraw-Hill New York.
17. Han, D.-h. and M.L. Batzle, *Gassmann's equation and fluid-saturation effects on seismic velocities.* Geophysics, 2004. **69**(2): p. 398-405.
18. Smith, T.M., C.H. Sondergeld, and C.S. Rai, *Gassmann fluid substitutions: A tutorial.* Geophysics, 2003. **68**(2): p. 430-440.
19. Carcione, J.M., et al., *Cross-hole electromagnetic and seismic modeling for CO2 detection and monitoring in a saline aquifer.* Journal of Petroleum Science and Engineering, 2012. **100**: p. 162-172.
20. Batzle, M. and Z. Wang, *Seismic properties of pore fluids.* Geophysics, 1992. **57**(11): p. 1396-1408.
21. Watt, J.P., *Hashin-Shtrikman bounds on the effective elastic moduli of polycrystals with orthorhombic symmetry.* Journal of Applied Physics, 1979. **50**(10): p. 6290-6295.
22. Hill, R., *Elastic properties of reinforced solids: some theoretical principles.* Journal of the Mechanics and Physics of Solids, 1963. **11**(5): p. 357-372.
23. Vera, V.C., *Seismic modelling of CO2 in a sandstone aquifer, Priddis, Alberta*. 2012, University of Calgary.